Journal of Photochemistry and Photobiology A: Chemistry 219 (2011) 50–57

Contents lists available at ScienceDirect

Journal of Photochemistry and Photobiology A: Chemistry

journal homepage: www.elsevier.com/locate/jphotochem

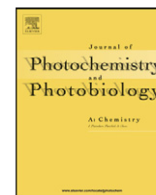

Research paper

Novel polymeric nonionic photoacid generators and corresponding polymer Langmuir–Blodgett (LB) films for photopatterning

Wenjian Xu[a], Tiesheng Li[a,*], Gaojian Li[a], Yangjie Wu[a,*], Tokuji Miyashita[b]

[a] Department of Chemistry, Zhengzhou University, The Key Lab of Chemical Biology and Organic Chemistry of Henan Province, The Key Lab of Advanced Nano-information Materials of Zhengzhou, Zhengzhou 450052, PR China
[b] Institute of Multidisciplinary Research for Advanced Materials, Tohoku University, 2-1-1 Katahira Aoba-ku, Sendai 980-8577, Japan

ARTICLE INFO

Article history:
Received 26 September 2010
Received in revised form 19 January 2011
Accepted 21 January 2011
Available online 1 February 2011

Keywords:
Photoacid generator
Langmuir–Blodgett films
Polymer resist
Photolithography
Photodegradation

ABSTRACT

A series of new polymeric nonionic photoacid generators (PAGs) and PAG-bound polymers designed for photoresist materials in Langmuir–Blodgett (LB) films have been synthesized and characterized. The novel polymer could form a stable and condensed monolayer on water surface, which could be transferred successfully onto solid substrate. Upon deep UV irradiation, the acid generated by the photoacid generator catalyzed the naphthyl moiety to liberate naphthol and regenerate carboxyl in the exposed region. The rent moiety could dissolve in alkaline aqueous, resulting in a fine positive tone resist patterns with a resolution of 0.75 μm. Sensitivity curves and TGA studies revealed that the high sensitivity in 248 nm irradiation was attributed to the present of PAG units incorporated in the polymer chains. The result of translated gold pattern with the same resolution as the resist pattern also demonstrated that the resist LB films had sufficient resistance to wet etching process.

© 2011 Published by Elsevier B.V.

1. Introduction

The microelectronic industry has made remarkable progress with the development of integrated circuit (IC) technology, which depends on the research efforts in a variety of high resolution lithography techniques, including exposure tools (electron beam, X-ray and deep UV technologies), sensitive resist materials system and appropriate film-forming methods. The major requirement for photoresists is that upon exposure to irradiation they undergo a structural change to provide solubility differentiation between the exposed and unexposed regions (controlled by mask). Chemically amplified (CA) resists is a promising class of materials for achieving high sensitivity and resolution [1–3]. In designing a resist system based on the chemical amplification concept, it has to incorporate two basic components, namely, an acid-labile compound or polymer and a photoacid generator (PAG) which should generate a strong acid by UV irradiation in solid state [4,5]. Recently, tremendous efforts have contributed towards the design and synthesis of new PAG for application in CA resist systems. Ionic PAGs enjoys several advantages such as high thermal stability, easily modified strength and size of the photogenerated acid [6,7]. Nonionic PAGs have a wide range of solubility in organic solvents and polymer film. It has been reported that the PAG blended CA resist materials have inherent incompatibility between polymer matrix and PAG, which can lead to PAG phase separation, PAG aggregation, nonuniform initial PAG and photoacid distribution, as well as acid migration during the post exposure baking (PEB) processes [8,9]. The best way to eliminate the problems associated with physically blended PAG/polymer resists is, perhaps, to incorporate the PAG units in the polymer chain to make PAG-bound resist, rather than physically blending the PAG with the polymer [10–12]. Wang et al. have reported that the incorporation of anionic PAG units into the main chain of the adamantly methacrylate based polymers showed faster photo speed, higher stability, lower outgassing and lower line edge roughness (LER), comparing with the PAG blended polymer resists [13–16]. Wu et al. have reported that the CA resists with cationic PAG unit in the polymer chain exhibited excellent film formation behavior due to absence of phase separation, which would often be observed in CA resists formulated by mixing a polymer matrix with small molecule PAGs [17,18]. Chung et al. attempted incorporation of camphorsulfonyl groups into a polymer chain by means of N-substitution in the maleimide monomer to provide high efficiency in photoacid generation and thermal stability [6]. Ahn et al. have reported the nonionic maleimide (MI) bound polymer has special physicochemical properties such as high thermal stability, high chemical resistance and low absorption in the deep-UV (DUV) region [6,19,20].

Ultra-thin films of photoresist less than 150 nm in thickness may be necessary to implement single layer photoresist

* Corresponding authors. Tel.: +86 371 67766667; fax: +86 371 67766667.
E-mail addresses: lts34@zzu.edu.cn (T. Li), wyj@zzu.edu.cn (Y. Wu).

1010-6030/$ – see front matter © 2011 Published by Elsevier B.V.
doi:10.1016/j.jphotochem.2011.01.015

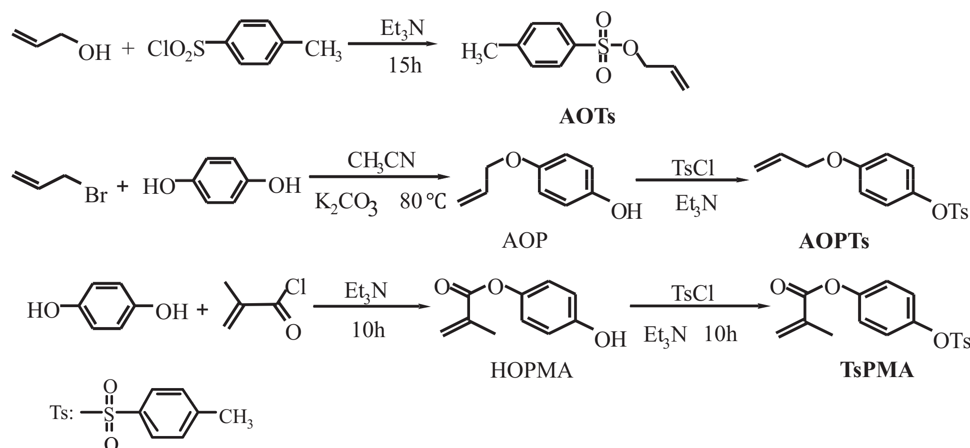

Fig. 1. Synthetic scheme of PAG monomers.

strategies for vacuum ultra-violet (VUV) and extreme ultraviolet (EUV) lithography [21,22]. In these wavelength regimes, light is strongly absorbed by most organic materials. The thickness of the resist film must therefore be reduced to maintain sufficient transparency to obtain high quality, anisotropic patterns. Langmuir–Blodgett (LB) technique is more advanced than the spin-coating and self-assembly in preparing a thin film with a controlled thickness at a molecular size and well-defined molecular orientation as well as the desquamation of resists from substrate [23,24]. So, just because of their superior features, polymer LB films have been recently investigated in the application to high-resolution lithographic technology [25–27]. However, CA resists LB films with PAGs in their chains have not received wide attention in the imaging industry, despite their potential advantages over their counterparts that are formulated by traditional spin-coating.

In this paper, we report a series of new polymeric nonionic PAGs and CA resists LB films with PAG units in the polymer main chain. The design of photoresist molecular was based on a methacrylate polymer backbone due to minimal deep UV absorbance: N-dodecylmethacrylamide (DDMA) was included in the microstructure to improve the film-forming [26]; β-naphthyl methacrylate (NPMA) was incorporated as the acid-cleavable bulky aromatic substituent groups to improve resolution, sensitivity and dry etch resistance [28]; allyl-4-methylbenzensulfonate (AOTs), 4-(allyloxy)phenyl-4-methbenzenesulfonate (AOPTs) and 4-(tosyloxy) phenyl methacrylate (TsPMA) (the synthesis schemes were outlined in Fig. 1) were bound in polymer chain as photoacid generator (PAG). The microstructure of terpolymer is outlined in Fig. 2. Considering these superior properties, we expect to improve not only the sensitivity but also the imaging quality of this new kind of resist system.

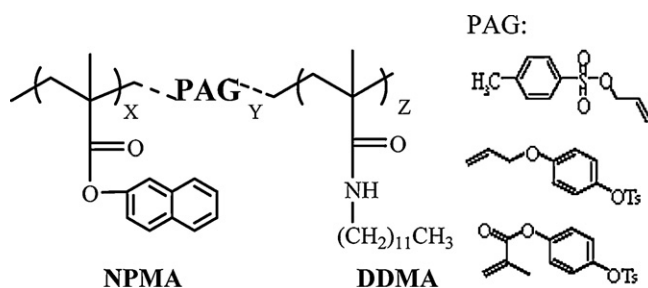

Fig. 2. Microstructure scheme of p(DDMA/NPMA/PAG).

2. Experimental

2.1. Synthesis of the PAG monomer

Three kinds of PAG monomer were synthesized by multistep procedure. The synthesis schemes were outlined in Fig. 1.

2.1.1. Synthesis of allyl-4-methylbenzensulfonate (AOTs)

AOTs was synthesized from p-toluenesulfonic chloride with allylalcohol in the presence of triethylamine and chloroform at 0 °C. After 15 h, the reaction mixture was washed three-times with NaCl aqueous solution. Then the organic layer, which was dried with anhydrous Na_2SO_4 overnight, was filtrated and concentrated to give the colorless oil. The crude product was purified by column chromatography (200–300 mesh of silica gel, eluted: acetic ether/petroleum ether = 1/6). Colorless oil was obtained after the solution was removed and dried under vacuum overnight. The yield was 78.3%. The ^{1}H NMR (400 MHz) data was given as follows: ($CDCl_3$, ppm) δ 2.44 (s, 3H), 4.47–4.48 (d, 2H), 5.29–5.30 (s, 1H), 5.40–5.41 (s, 1H), 5.98–6.03 (d, 2H), 6.78–6.79 (d, 2H), 6.85–6.86(d, 2H), 7.29–7.31 (d, 2H), 7.67–7.69 (d, 2H). FT-IR (cm^{-1}): 3031 (υ_{C-H} of -benzene), 2929 (υ_{C-H} of ane), 1494, 1598 ($\upsilon_{C=C}$ of benzene), 1421 (υ_{as} of $-CH_3$), 1363 (υ_{-SO2-} of ester), 10782 (υ_{S-O-C} of ester). MS (EI) m/z: 233 (M + H).

2.1.2. Synthesis of 4-allyloxyphenol (AOP)

A mixture of hydroquinone allyl bromide, anhydrous potassium carbonate and acetonitrile was refluxed for 12 h and cooled. The reaction mixture was filtrated and concentrated. It was diluted with 50 mL dichloromethane, and washed once with 1 N HCl aqueous solution and twice NaCl aqueous solution. Then the organic layer, which was dried with anhydrous Na_2SO_4 overnight, was filtrated and concentrated to give the brown oil. The crude product was purified by column chromatography (200–300 mesh of silica gel, eluted: acetic ether/petroleum ether = 1/5). Brown oil was obtained after the solution was removed and dried under vacuum overnight. The yield was 31.6%. The ^{1}H NMR (400 MHz) data was given as follows: ($CDCl_3$, ppm) δ 4.47–4.48 (d, 2H), 5.26–5.29 (s, 1H), 5.37 (s, 1H), 5.42 (d, 1H), 5.99–6.07 (m, 1H), 6.75–6.84 (q, 2H). FT-IR (cm^{-1}): 3403 (υ_{C-H} of O–H), 3027 (υ_{C-H} of benzene), 2983, 2925 (υ_{C-H} of ane), 1644 ($\upsilon_{C=C}$ of ene), 1453, 1506, 1608 ($\upsilon_{C=C}$ of benzene), 1359 (υ_{as} of $-CH_3$), 1092 (υ_{C-O-C} of ether). MS (EI) m/z: 151 (M + H).

2.1.3. Synthesis of 4-(allyloxy) phenyl-4-methbenzenesulfonate (AOPTs)

A mixture of 4-allyloxyphenol (AOP), p-toluenesulfonic chloride, triethylamine and chloroform was stirred for 10 h at 0 °C. A

Table 1
Polymerization results of terpolymer.

Polymer	Compositions (in polymer*)		mol.%	Mn	Mw	PDI	Yield
	DDMA	NPMA	TsPMA	$(\times 10^4)$	$(\times 10^4)$		%
a	80(58.2)	10(32.3)	10(9.5)	0.84	3.04	3.62	78.1
b	70(63.9)	20(19.6)	10(16.5)	1.23	3.26	2.56	75.3
c	60(67.5)	20(17.1)	20(15.4)	1.09	5.12	4.68	86.2
d	50(50.0)	20(25.0)	30(25.0)	1.38	3.24	2.35	80.1

* Measured with ^{1}H NMR.

series of purification procedure were done as the method of *AOP*. Brown solid was obtained at a yield of 99.2%. mp: 47–48 °C. The ^{1}H NMR (400 MHz) data was given as follows: ($CDCl_3$, ppm) δ 2.44 (s, 3H), 4.47–4.48 (d, 2H), 5.29–5.30 (s, 1H), 5.40–5.41 (s, 1H), 5.98–6.03 (m, 1H), 6.78–6.79 (d, 2H), 6.85–6.86 (d, 2H), 7.29–7.31 (d, 2H), 7.67–7.69 (d, 2H). FT-IR (cm^{-1}): 3070 (υ_{C-H} of benzene), 2983, 2925 (υ_{C-H}), 1704 ($\upsilon_{C=O}$ of ester), 1648 ($\upsilon_{C=C}$ of ene), 1461, 1502, 1596 ($\upsilon_{C=C}$ of benzene), 1421 (υ_{as} of $-CH_3$), 1639 (υ_{-SO2-} of ester), 1092 (υ_{C-O-C} of ester), 1013 (υ_{C-O-C} of ether). MS (EI) *m*/*z*: 327 (M + Na).

2.1.4. Synthesis of 4-hydroxyphenyl methacrylate (HOPMA)

HOPMA was prepared by reacting methacryloyl chloride with the hydroquinone in the presence of triethylamine and chloroform at 0 °C. α-Methacryloyl chloride in 15 mL of anhydrous chloroform was dropwisely added in 50 mL of hydroquinone chloroform with 20 g hydroquinone solution at 0 °C. The mixture was stirred at room temperature for 10 h and poured into 1 N HCl ice water containing NaCl. The organic layer, which was dried with anhydrous Na_2SO_4 overnight, was filtrated and concentrated to give the pale-yellow solid. The crude product was purified by column chromatography (200–300 mesh of gel, eluted: acetic ether/petroleum ether = 1/5). A pale-yellow crystalloid was obtained after the solution was removed and dried under vacuum overnight. Yield: 35.7%, mp: 119–120 °C. The ^{1}H NMR (400 MHz) data was given as follows: ($CDCl_3$, ppm) δ 2.06 (s, 3H), 2.19 (s, 1H), 5.76 (s, 1H), 6.35 (s, 1H), 6.72–6.75 (d, 2H), 6.90–6.93 (d, 2H). FT-IR (cm^{-1}): 3459 (υ_{O-H}), 3033 (υ_{C-H} of benzene), 2955, 2924 (υ_{C-H}), 1708 ($\upsilon_{C=O}$ of ester), 1633 ($\upsilon_{C=C}$ of ene), 1441, 1507, 1588 ($\upsilon_{C=C}$ of benzene), 1009 (υ_{C-O-C} of ester). MS (EI) *m*/*z*: 176.8 (M − 1).

2.1.5. Synthesis of 4-(tosyloxy) phenyl methacrylate (TsPMA)

TsPMA was synthesized from p-toluenesulfonic chloride with 4-mathacrylocoxyphenol (MAOP) in the presence of triethylamine and chloroform at 0 °C. After 10 h, the reaction mixture was washed twice with NaCl aqueous solution. Then the organic layer, which was dried with anhydrous Na_2SO_4 overnight, was filtrated and concentrated to give the pale yellow solid. The crude product was purified by column chromatography (200–300 mesh of gel, eluted: acetic ether/petroleum ether = 1/5). A pale yellow crystalloid was obtained after the solution was removed and dried under vacuum overnight. Yield: 98.6%, mp: 78–79 °C. The ^{1}H NMR (400 MHz) data was given as follows: ($CDCl_3$, ppm) δ 2.04 (s, 3H), 2.45 (s, 3H), 5.77 (s, 1H), 6.33 (s, 1H), 6.98–7.00 (d, 2H), 7.04–7.06 (d, 2H), 7.31–7.33(d, 2H), 7.70–7.22 (d, 2H). FT-IR (cm^{-1}): 3070 (υ_{C-H} of benzene), 2962 (υ_{C-H} of ane), 1735 ($\upsilon_{C=O}$ of ester), 1633 ($\upsilon_{C=C}$ of ene), 1454, 1500, 1596 ($\upsilon_{C=C}$ of benzene), 1373($C_{s=O_2}$ of ester). MS (EI) *m*/*z*: 355.1 (M + Na).

2.2. Synthesis of polymers

Both homo and copolymerization were carried out by conventional free radical polymerization with AIBN as initiator. The *N*-dodecylmethacrylamide (DDMA) and β-naphthyl methacrylate (NPMA) was synthesized as the methods mentioned in the literature [26,28]. A typical procedure was as follow: the monomers and 1 wt% initiator respect to monomer (including PAG monomer) were dissolved in dioxane. The solution was filtered through a 0.45 μm Teflon micro filter into a sealed flask. N_2 in-pump-out cycles were run three times to remove oxygen. The clear solution was then placed in a 60 °C water bath under stirring. The reaction was maintained under nitrogen for 24 h. The polymer was isolated by pouring the reaction solution into sufficient amount of n-hexane with vigorous stirring, filtered and washed thoroughly with hexane. Then the polymer was purified by redissolving in acetone and reprecipitating from distilled and deionized water or methanol. Finally, the polymer was dried in vacuum at 50 °C over night. In this way, PAG homopolymers pTsPMA and terpolymer p(DDMA/NPMA/TsPMA) were prepared respectively. Table 1 lists the characteristic data of p(DDMA/NPMA/TsPMA).

2.3. Materials and characterization

Hydroxylamine, acetone, methanol, hexane, THF (tetrahydronfunan), p-Hydroquinone (HQ), and maleic anhydride were purchased from Tianjin Chemical Reagents. Furan, 2, 2′-azobisisobutyronitrile (AIBN), rhodamine B base (RB) and p-toluenesulfonic chloride were purchased from China National Medicine Co. Other chemicals were purified by conventional methods.

^{1}H NMR was measured with NMR DPX-400 (Bruker, German) in $CDCl_3$. UV–visible absorption spectrum was obtained on Lambda 35 UV–Visible spectrophotometer (Perkin Elmer Inc., USA). Infrared spectra were obtained with Bruker Vector-22. Deep UV irradiation was carried out with EX250 UV light source (Honya-Schott Ltd., Japan). The molecular weight was determined by PL-GPC 50 in tetrahydrofuran (THF) with polystyrene standards. Thermogravimetric analysis (TGA) was obtained on NETSCH TG 209 in N_2 atmosphere. Photopatternings were observed by microscope (OLYMPUS BX51, OLYMPUS Co., Japan). The thickness of thin film was determined with an Optical Thin Film Analysis System NKD-8000v (Aquila Instruments Ltd., UK).

Measurement of surface pressure (π)–area (A) isotherms and the deposition of monolayer were carried out with a computer controlled Langmuir–Blodgett system (KSV-5000-3, KSV Instruments, Helsinki, Finland) at a compression speed of 10 mm/min. Distilled and deionized water with resistivity of 18.2 MΩ cm (MILI-Q gradient MILIPORE CO., USA) was used for subphase. The terpolymer was dissolved in chloroform at a concentration of approximately 0.5 mg/mL and the solution was spread on the water surface by a micrometric syringe. Waiting for about 30 min to let the solvent evaporate out, the monolayer compression started at a compression rate of 10 mm min^{-1}. The isotherms for every sample were measured for twice to ensure good reproducibility. Quartz, glass and silicon substrate slides used for LB films deposition were prepared by being treated with boiling concentrated HNO_3 solution, and then washed with water to ensure its hydrophile. All measurements were carried out at room temperature.

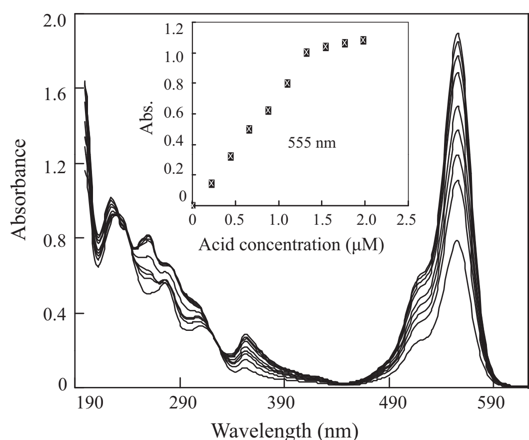

Fig. 3. Absorption spectra of rhodamine B base without and with varying amounts of 4-methylbenesulfonic acid in acetonitrile at room temperature. Inset: absorption at 555 nm as a function of the acid concentrations.

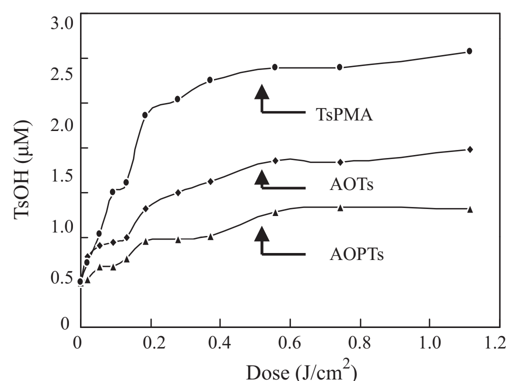

Fig. 4. Acid generation efficiency vs. doses for PAG monomer in acetonitrile.

3. Results and discussion

3.1. Acid generating efficiency measurements

The acid generating efficiency of the monomers and polymers were measured by xanthene dyes rhodamine B base (RB) [29]. To calibrate the absorption of RB, varying amounts of 4-methylbenesulfonic acid and RB stock solution ($C_{RB} = 2.8 \times 10^{-5}$ mol L^{-1}) were placed in a 4 mL quartz cell. The corresponding UV–visible spectra were recorded on a Perkin-Elmer Lambda 35 spectrophotometer, in which acetonitrile was taken as reference. The absorption maximum at 555 nm was measured on the spectra. In Fig. 3, bulky line showed the UV–visible spectra RB in acetonitrile as a function of 4-methylbenesulfonic acid concentrations. The absorbance increasing at 555 nm was caused by successive addition of 4-methylbenesulfonic acid to the solution in 0.022 μmol increments. A straight line was obtained when absorbance at 555 nm was plotted as a function of the acid concentrations, as shown in Fig. 3 inset, which can be used as calibration curves for determining the acid concentrations of PAG.

To measure the acid generation efficiency of the PAG-bound polymers, films were casted on 30 mm × 30 mm quartz plate whose weights were predetermined on an analytical balance, from 10 wt% solutions in acetone. Then polymer films were baked at 90 °C for 5 min to remove the solvent and weighted again. The amount of polymer in film was calculated. Then the polymer film was exposed to 248 nm DUV radiations for varying length of time. Doses were calculated by multiplying exposure times by lamp intensity. The exposed film was immediately stripped from the plate with acetonitrile and collected in a 20 mL measuring flask. It was added 2.8×10^{-5} mol L^{-1} RB stock solution. The total volume was then raised to 20 mL by addition of acetonitrile. The UV–visible spectrum of the resulting solution was obtained using acetonitrile as reference. The amount of acid generated in film by UV radiation was determined by measuring the absorbance at 555 nm and comparing with the calibration curve.

Copolymer samples contained PAG were designed as potential CA resists. As discussed earlier [13–16], the acid generation efficiency of PAG in a polymer/PAG blend was highly dependent on the miscibility of the polymer and the PAG. In the present case, acid generating units were incorporated into the polymer chains for polymers **a–d**. Therefore the acid generation efficiency for these polymers was determined.

The acid generation efficiency of these polymers was measured by the rhodamine B base (RB) method using 248 nm DUV as a radiation source. Since the polymers contain varying amounts of the acid generating units, comparison of the acid generating efficiency for each polymer was expressed as mole of TsOH acid per mole of the PAG units in the polymer. The number of moles of the PAG units in each polymer was determined by ^{1}H NMR.

Fig. 4 showed the results obtained from the PAG monomers of AOTs, AOPTs and TsPMA in acetonitrile. In all cases, the acid generation efficiency increased as the doses of radiation applied. Surprisingly, all samples followed a similar pattern, which suggested that they had the same acid generating mechanism depended on irradiation dose. At the forepart of irradiation, the acid generation efficiency rose rapidly until 200 mJ/cm^2, and then underwent a slow growth. TsPMA had the highest acid yield among of them. So a series of copolymer film contained PAG monomer TsPMA had been used to measure the acid generation efficiency as follow.

Fig. 5 showed the results obtained for copolymers **b–d**. In all cases, the acid generation efficiency increased with doses of radiation applied. All three samples followed a similar pattern, viz. there was a down fold around 50 mJ/cm^2 in the slow climbing curve of acid generation efficiency vs. dose of radiation.

The possible explanation is generated to interpret their different demonstration as follows. It had been well reported that the sensitivity of radiation-sensitive compound usually depended on its environment. While the radiation-sensitive groups in such a compound could absorb energy directly from radiation, and they could obtain energy indirectly from its neighbor as well, which is called as energy transfer. Unlike a discrete PAG, the PAG units in polymer **d** were probably incorporated into the polymer chains and therefore could absorb energy from neighboring repeating units. This

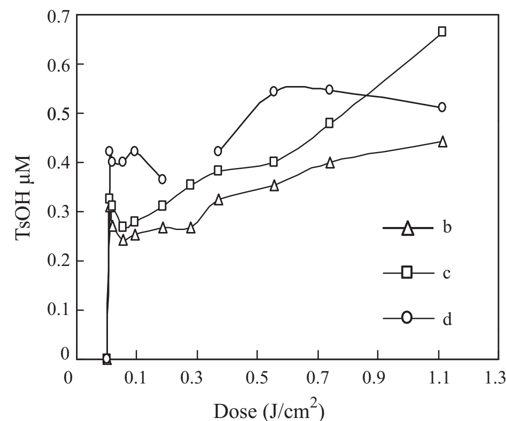

Fig. 5. Acid generation efficiency vs. doses for the thin film of p(DDMA/NPMA/TsPMA).

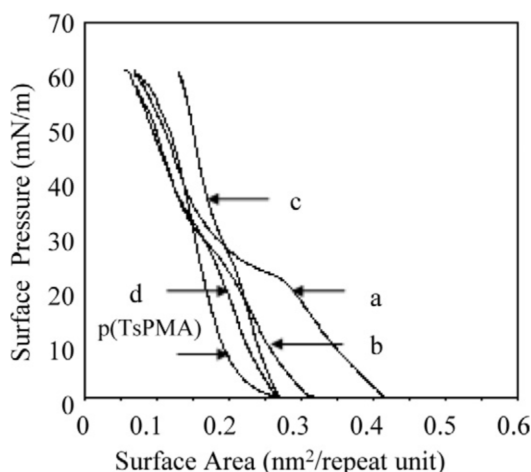

Fig. 6. Surface pressure–area isotherms of the PAG-copolymer on the water surface at 25 °C with a compression rate of 10 mm/min.

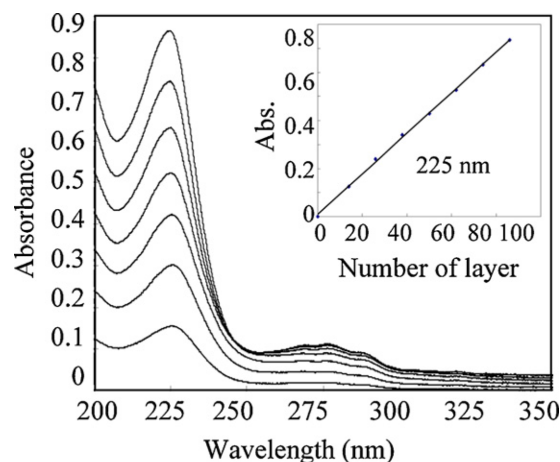

Fig. 8. UV absorption of PAG-copolymer **b** LB films as a function of the number of deposited layers. Inset: plots of the absorbance at 225 nm vs. the number of LB films deposited.

additional energy could assist in fission of oxygen–sulfur bonds that were necessary for acid generation. More importantly, since the photo-induced acid generation from a sulfonic group involved a hydrogen-abstracting process, these neighboring repeating units provided much more abundant hydrogen resource to the sulfonic groups. Maybe this was not the case with a polymer/PAG blend.

3.2. Behavior of monolayer and LB films formation at the air/water interface for PAG-bound copolymers

Fig. 6 showed the surface pressure (π)–area (A) isotherms of Langmuir monolayer of p(DDMA/NPMA/TsPMA) copolymers. For comparison, the isotherm of TsPMA homopolymer (pTsPMA) was also shown in Fig. 6. The (π)–area (A) isotherms of PAG-bound copolymer with various compositions showed that all the copolymers formed stable monolayer on water surface under a high surface pressure (π). Compared with copolymer, the curve of PAG homopolymer showed the best ability of forming more stable monolayer with the highest collapse pressure (50 mN/m). This maybe attribute to the big steric hindrance of naphthyl side group in the copolymers.

The static elasticity (E_s)–surface pressure (π) isotherm [30] of p(DDMA/NPMA/TsPMA) with various TsPMA had been studied (Fig. 7). For each E_s–π curve in Fig. 7, two peaks appeared in the liquid-expanded and the liquid-condensed section respectively. The isotherm of PAG homopolymer demonstrated the widest peak, and the **c** gave the highest peak value. All of them will be profitable for achieving optimum conditions for LB films deposition of terpolymer monolayer.

The multilayer transfer behavior of the copolymer monolayer was examined by UV–visible spectra. Fig. 8 showed the UV–visible absorbance of the **b** LB films as a function of the number of deposited LB films on quartz substrate at 25 mN/m (with a total average transfer ratio of 0.9 in upward stroke). The absorbance at 225 nm was proportion to the number of layers at least up to 90 layers. The linear relationship between the absorbance and the number of layers suggested that a regular deposition of the copolymer monolayer took place (Fig. 8 inset), resulting in a fair uniform LB films. Fig. 9 showed plots of the absorbance at 225 nm vs. the number of LB films deposited for TsPMA copolymer **a**, **b**, **c** and **d**. All of these indicated that the LB films of PAG-bound copolymer were ordered film with well-defined architecture.

3.3. Decomposition of p(DDMA/NPMMA/TsPMA) Induced by deep UV light

Fig. 10 showed the change of UV absorption spectra of p(DDMA/NPMMA/TsPMA) **c** LB films with 86 layers deposited onto quartz following deep UV irradiation. The maximum absorbance at 196 nm and 225 nm, which can be assigned to the characteris-

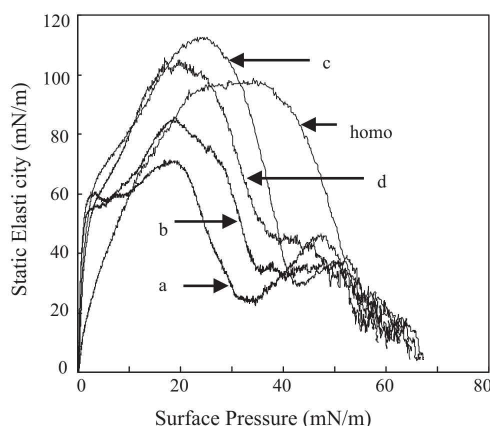

Fig. 7. The static elasticity as a function of surface pressure on water surface at 25 °C for p(DDMA/NPMA/TsPMA).

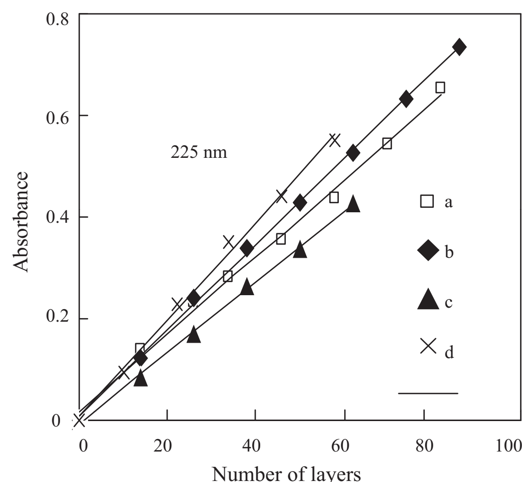

Fig. 9. Plots of the absorbance at 225 nm vs. the number of LB films deposited for PAG-containing copolymer.

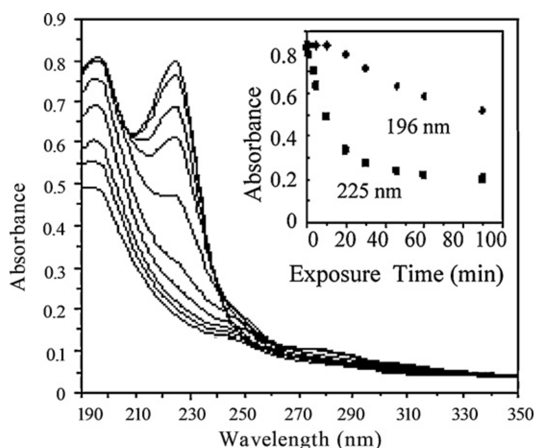

Fig. 10. UV absorption spectra for the LB films of p(DDMA/NPMA/TsPMA)s **c** LB films with 86 layers on a quartz at different irradiating times. Insert: relationship between absorbance and irradiation time at 196 and 224 nm.

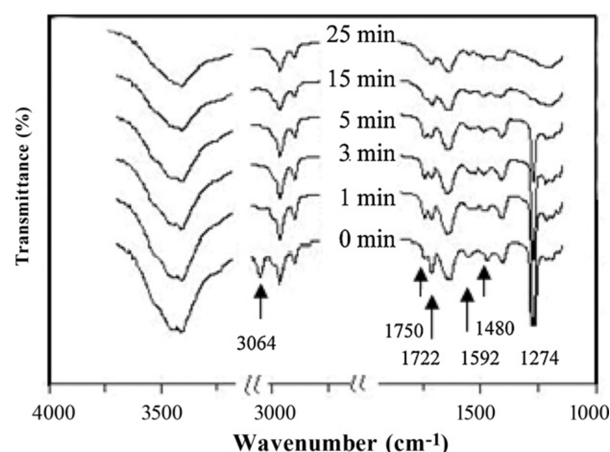

Fig. 12. Change of IR spectra of terpolymer p(DDMA/NPMA/TsPMA)s **c** casting membrane, which were deposited on KBr tablet, irradiated by deep UV light for 0, 1, 3, 5, 15 and 25 min.

tic absorption of benzene and naphthalene ring, decreased with the increasing irradiation time. Apparently, upon irradiation, the LB films underwent photodegradation of polymer side chain. The absorbance decreasing in such a short time indicated that the LB films of p(DDMA/NPMA/TsPMA)s were sensitive to deep UV light.

The sensitivity curves were measured for the samples of p(DDMA/NPMA) (0 mol.% TsPMA), p(DDMA/NPMMA/TsPMA17) (16.5 mol.% TsPMA), p(DDMA/NPMMA/TsPMA25) (25.0 mol.% TsPMA) LB films with 39 layers. The residual thickness of the LB films in the exposed portion was measured as a function of the exposure time (Fig. 11). The results of the normalized film thickness decreasing with increasing exposure time showed they were the typical positive type resist, i.e., the irradiation region of copolymer LB film was effectively decomposed by deep UV irradiation and removed completely with a developer of alkaline aqueous (TMAH). It was clear that due to the presence of the PAG, the sensitivity of PAG containing terpolymer was higher than that of p(DDMA/NPMA) under the same condition. It was also found that due to the number of Ts group increased, the sensitivity was remarkably enhanced with the mole fraction of PAG.

Infrared spectroscopy was employed to investigate the change of the photodegradable properties of PAG terpolymer film by deep UV irradiation. Fig. 12 showed the infrared spectrum of terpolymers p(DDMA/NPMA/TsPMA)s **c** thin films, which was cast on a

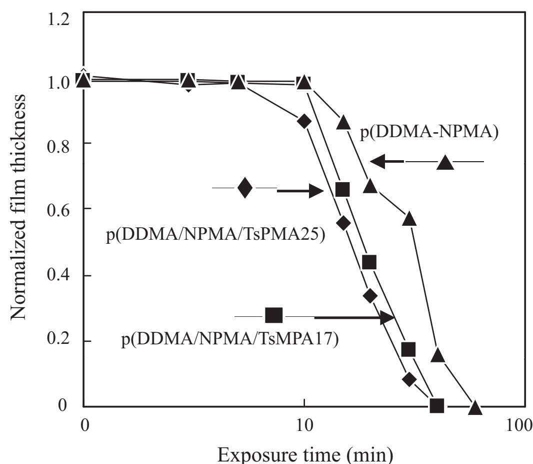

Fig. 11. Sensitivity curves of p(DDMA-NPMA) and p(DDMA/NPMA/TsPMA) thin film irradiated by deep UV light followed by developed with 1% TMAH for 20 s. PEB temperature: 90 °C for 30 s.

KBr tablet. The peak at 1274 cm^{-1} assigned to the stretching vibration of SOO moiety of sulphonate decreased with irradiation time increasing and disappeared after UV irradiation for 15 min, which confirmed that the destruction of the sulphonate unit happened in side chain of polymer. The destruction of the benzene and naphthalene ring was confirmed by the disappearance of weak bands at 1480 cm^{-1} and 1592 cm^{-1}, which were assigned to the characteristic frequency for a skeletal in-plane vibration of the benzene and naphthalene ring. Meanwhile, the peaks at 3064 cm^{-1} assigned to the stretching vibration of C-H in aromatic nucleus disappeared after 248 nm UV irradiation 1 min, which could also be seen from the IR spectra. All the results indicated that the sulphonate was decomposed and new functional group was produced, such as –COOH or –OH. Absorbance at approximately 3400 cm^{-1}, assigned to the stretching vibration group of N-H, free (non-associated) and hydrogen bonded hydroxyl/hydroperoxide group, was decreased with increasing irradiation time. The phenomenon could be seen in the UV spectrum of terpolymer p(DDMA/NPMA/TsPMA)s **c** as shown in Fig. 10. Moreover, the peaks at 1750 cm^{-1} assigned to the stretching vibration of C=O decreased, which was assigned to the carbonyl group weakened by the deep UV irradiation. This also meant that the benzene and naphthalene ring group was removed from the side chain to give a phenol group so that the residual could be dissolved in alkaline solution. Such decrease involved not only the side groups but also the backbone structure, as shown by the spectral changes in the zone of –C–H stretching of CH_2/CH_3 groups, 2850–3000 cm^{-1}. Key to the chemical amplification feature of this resist was the fact that proton that initiates the overall reaction sequence was not lost, which then became available for additional deprotection. PAG can generate proton when irradiated by UV light, so it can catalyze the deprotection of photoresist.

3.4. Thermal stability of polymer containing PAG

One basic requirement for CA resist is that it must be thermally stable [19]. Fig. 13 illustrated the effect of the thermal stability of homopolymer pTsPMA (curve 1 and 2), terpolymer pDDMA/NPMA/TsPMA (curve 3 and 4) and copolymer pDDMA/NPMA (curve 5 and 6) before and after DUV irradiation. TGA was used to follow the weight loss associated with the thermolysis of the naphthyl group from the polymer backbone. Upon thermal decomposition, the naphthyl moiety liberated naphthyl alcohol and other derivant. To determine the comparative effect, TsPMA on the thermolysis of the naphthyl group different molar of the sulfonate ester 100 (pTsPMA), 15.4 (terpolymer

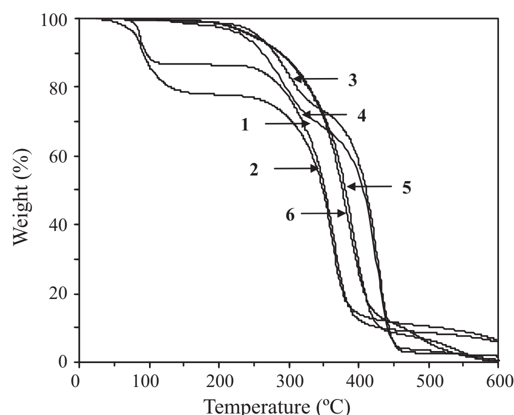

Fig. 13. TGA of terpolymer p(DDMA/NPMA/TsPMA)s **c**, copolymer p(DDMA/NPMA 50) and homopolymer p(TsPMA) (**1**) homopolymer p(TsPMA) before (**2**) after exposure to 250 nm UV for 60 min; (**3**) terpolymer p(DDMA/NPMA/TsPMA)s before (**4**) after exposure to UV light for 60 min; (**5**) copolymer p(DDMA/NPMA 50) before (**6**) after exposure to UV light for 60 min.

Fig. 14. Optical micrograph of positive fine patterns with p(DDMA/NPMA/TsPMA)s **c** LB film 35 layers on a glass substrate after UV irradiation following development with 1% TMAH aqueous solution.

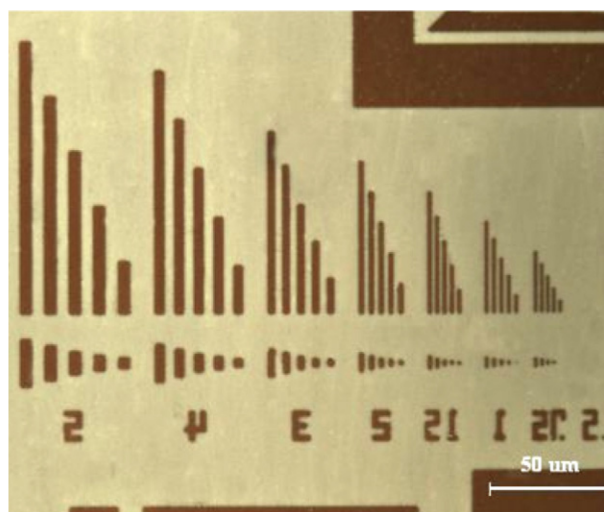

Fig. 15. Optical micrograph of etched pattern of gold film on glass substrate.

c) and 0 (pDDMA/NPMA50) mol.% relative to polymer were monitored. The TGA result indicated that the deprotection temperature (T_{dp}) was decreased with increasing the amount of TsPMA in copolymer before exposing, which showed the sequence of T_{dp} (pTsPMA) < T_{dp} (pDDMA/NPMA/TsPMA) < T_{dp} (pDDMA/NPMA50) as shown in Fig. 13. The deprotection temperature of copolymer had obvious phenomenon after irradiated by 248 nm light for 60 min. This reduction in the thermolysis temperature of the naphthyl group verified that acidic species was liberated upon the decomposition of TsPMA in copolymer. For the first, the DUV irradiation of p(DDMA/NPM/TsPMA)s resulted in generation of the corresponding *p*-toluenesulfonic acid, which catalyzed the deprotection of naphthyl groups. As seen from Fig. 13, the temperature of deprotection of naphthyl functionalized was greatly reduced by comparing with (**1**) and (**2**), (**3**) and (**4**). It had a smaller effect on the temperature of deprotection of pDDMA/NPMA50 before and after irradiation, because there was no TsPMA in copolymer (i.e., no amount of acid was formed). The TGA studies showed that the thermal stability of the terpolymers p(DDMA-NPMA-TsPMA)s greatly decreased with an increase of the number TsPMA units in the copolymer chain irradiated by deep UV light and increased without irradiation. We could deduce that the sensitivity of p(DDMA/NPMA/TsPMA)s could be improved by introducing TsPMA group into the main chain of p(DDMA/NPMA).

3.5. Photopatterning of polymers containing PAG

The p(DDMA-NPMA-TsPMA)s **c** LB films with 35 layers were deposited on glass-gilded substrate, irradiated by 248 nm UV light source in air through a photomask for 20 min, and then were developed in 1% aqueous solution of tetramethyl ammonium hydroxide (TMAH) for 10 s. The patterns of resists LB films were obtained as shown in Fig. 14. This microscopic image showed that the masked region of resist LB films was not dissolved, while the irradiated part was dissolved in 1% (TMAH) aqueous solution due to the chain scission, resulting in the decrease in the molecular weight as mentioned above. The maximum resolution of the resist pattern was 0.75 μm line-and-space, which was the highest resolution of the photomask employed in this study. Obviously, p(DDMA/NPMA/TsPMA) was a typical positive-tone photoresist, and this copolymer LB films was effectively decomposed by deep UV irradiation and completely removed with a developer of alkaline solution.

From the experiment results obtained above, fine positive-type patterns of p(DDMA/NPMA/TsPMA) LB films could be drawn. However, in lithography process the subsequent pattern transferring is the most important step. Thus, the etch resistance of films is also the critical factor just as sensitivity and resolution. Therefore, the polymer films employed in microlithography must have sufficiently resistance to wet etching or dry etching (plasma). The fine resist pattern obtained above was etched by immersing it in a mixed solution of iodine (0.6 g), ammonium iodide (1.5 g), ethanol (20 mL) and pure water (30 mL) for 20 s in order to remove the gold film uncovered by the resist LB film. Finally, the p(DDMA/NPMA/TsPMA) resists LB films were removed by chloroform for 20 s. Fine gold film pattern with the same resolution as that of the resist pattern was drawn as shown in Fig. 15. It can be observed that the surface of sample was smooth and clear-cut and the gold pattern had the maximum resolution of 0.75 μm as same as the resist pattern. These results indicated that the resist pattern was translated into gold pattern completely and the resist LB films had a high resistance to the wet enchant. Therefore, p(DDMA/NPMA/TsPMA)s LB films have a potential application to microfabrication.

4. Conclusion

A series of novel functionalized nonionic photo-acid generator, including 4-(tosyloxy)phenyl methacrylate (TsPMA),

allyl-4-methylbenzensulfonate (AOTs), 4-(allyloxy) phenyl-4-methbenzene- sulfonate (AOPTs) as well as corresponding PAG bound polymer resist, were prepared and characterized. A new approach of acid generating efficiency measurement was also employed. The terpolymers could form a stable, condensed monolayer on the water surface and could be transferred successfully onto solid supports, due to the absence of phase separation. The p(DDMA/NPMA/TsPMA)s functioned as novel CA resist with PAGs incorporated in the polymer chain. Preliminary results showed that terpolymer **c** LB films were successfully applied to photopatterning and the fine resist patterns with the resolution of 0.75 μm was yielded, which was the limit resolution of the photomask employed. High sensitivity of resist in 248 nm irradiation was attributed to the present of PAG units incorporated in the polymer chains. The result of translated gold pattern with maximum resolution also demonstrated that the resist LB films had sufficient resistance to a wet etching process. UV, IR and TGA spectra studies revealed that the formation of the pattern was attributed to the scission of the main chain and the cleavage of the side chain in LB films. Subsequently, a positive-tone pattern with high resolution was figured. The photopatterning properties and high resistance ability of terpolymers p(DDMA/NPMA/TsPMA)s LB films are expected to be applied as a photoacid-generating photoresist in ultra-thin photoresist and the fabrication of nano-filter as well as nano-tube.

Acknowledgements

This work is supported by the Innovation Fund for Outstanding Scholar of Henan Province (0621001100), the Natural Science Foundation of Henan Province (0611020100) and the Innovation Fund for Outstanding Youth of Henane Province (074100510015).

References

[1] H. Ito, Chemical amplification resists for microlithography, Adv. Polym. Sci. 172 (2005) 37–245.
[2] H. Ito, Chemical amplification resists: history and development within IBM, IBM J. Res. Dev. 44 (2000) 119–130.
[3] S.-Y. Moon, J.-M. Kim, Chemistry of photo-lithographic imaging materials based on the chemical amplification concept, J. Photochem. Photobiol. C: Photochem. Rev. 8 (2008) 157–173.
[4] T. Fujimori, S. Tan, T. Aoai, F. Nishiyama, T. Yamanaka, M. Momota, S. Kanna, Y. Kawabe, M. Yagihara, T. Kokubo, S. Malik, L. Ferreira, Structural design of a new class of acetal polymer for DUV resists, Proc. SPIE 3999 (2000) 579–590.
[5] A.M. Azam, K.E. Gonsalves, V. Golovkina, F. Cerrina, High sensitivity nanocomposite resists for EUV lithography, Microelectron. Eng. 65 (2003) 454–462.
[6] C.-M. Chung, K.-D. Ahn, Photochemical acid generation from copolymers based on camphorsulfonyloxymaleimide and acidolytic deprotection, React. Funct. Polym. 40 (1999) 1–12.
[7] M. Shiraia, M. Endo, M. Tsunooka, M. Endo, Highly sensitive positive surface modification resists, Microelectron. Eng. 53 (2000) 475–478.
[8] M. Shiral, M. Tsunooka, Photo-acid and photobase generators: chemistry and applications to polymeric materials, Prog. Polym. Sci. 21 (1996) 1–45.
[9] M. Shiral, T. Sumino, M. Tsunooka, Polysiloxane formation at the irradiated surface of polymers containing both photoacid generating units and epoxy unites, Eur. Polym. J. 33 (1997) 1255–1262.
[10] M.D. Stewart, H.V. Tran, G.M. Schmid, T.B. Stachowiak, D.J. Becker, C.G. Willson, Acid catalyst mobility in resist resins, J. Vac. Sci. Technol. B 20 (2002) 2946–2952.
[11] D. He, H. Solak, W. Li, F. Cerrina, Extreme ultraviolet and x-ray resist: comparison study, J. Vac. Sci. Technol. B 17 (1999) 3379–3383.
[12] D. Yang, S.W. Chang, C.K. Ober, Molecular glass photoresists for advanced lithography, J. Mater. Chem. 16 (2006) 1693–1696.
[13] M. Wang, W. Yueh, K.E. Gonsalves, Novel ionic photoacid generators (PAGs) and corresponding PAG bound polymers, J. Photopolym. Sci. Technol. 20 (2007) 751–755.
[14] M. Wang, N.D. Jarnagin, C. Lee, C.L. Henderson, W. Yueh, J.M. Roberts, K.E. Gonsalves, Novel polymeric anionic photoacid generators (PAGs) and corresponding polymers for 193 nm lithography, J. Mater. Chem. 16 (2006) 3701–3707.
[15] M. Wang, W. Yueh, K.E. Gonsalves, New anionic photoacid generator bound polymer resists for EUV lithography, Macromolecules 40 (2007) 8220–8224.
[16] M. Wang, N.D. Jarnagin, W. Yueh, J.M. Roberts, M. Tapia, N. Batina, K. EGonsalves, Novel polymeric anionic photoacid generators (PAGs) and photoresists for sub-100 nm patterning by 193 nm lithography, Proc. SPIE 6519 (2007) 65192C.
[17] H. Wu, K.E. Gonsalves, Preparation of a photoacid generating monomer and its application in lithography, Adv. Funct. Mater. 11 (2001) 271–276.
[18] H. Wu, K.E. Gonsalves, A novel single-component negative resist for DUV and electron beam lithography, Adv. Mater. 13 (2001) 195–197.
[19] K.-D. Ahn, C.-M. Chung, D.-H. Koo, Nevol functional polymers from N-(Tosyloxy) maleimide photochemical acid ceneration in solid-state and application as resist materials, Chem. Mater. 6 (1994) 1452–11452.
[20] K.-D. Ahn, D.-H. Koo, C.G. Willson, Synthesis and polymerization of t-BOC protected maleimide monomers: N-(t-butyloxycarbonyloxy) maleimide and N-[p-(t-butyloxycarbonyloxy) phenyl] maleimide, Polymer 36 (1995) 2621–2628.
[21] F.M. Houlihan, G.I. Dabbagh, R. Hutton, K. Bolan, E. Reichmanis, O. Nalamasu, Z. Yan, A. Reiser, Fundamental studies of dissolution inhibition in poly(norbornene-alt-maleic anhydride) based resins, Radiat. Phys. Chem. 62 (2001) 69–76.
[22] M.A. Ali, K. Gonsalves, V. Golovkina, F. Cerrina, High sensitivity nanocomposite resists for EUV lithography, Microelectron. Eng. 65 (2003) 454–462.
[23] A. Ulman, Function and structure of self-assembled monolayers, Chem. Rev. 96 (1996) 1533–1554.
[24] T. Miyashita, Recent studies on functional ultrathin polymer films prepared by the Langmuir–Blodgett technique, Prog. Polym. Sci. 18 (1993) 263–294.
[25] T.S. Li, M. Mitsuishi, T. Miyashita, Photolitho-graphic properties of ultrathin polymer Langmuir–Blodgett films containing anthracene moieties, J. Mater. Chem. 13 (2003) 1565–1569.
[26] T.S. Li, M. Mitsuishi, T. Miyashita, Ultrathin polymer Langmuir–Blodgett films for microlithography, Thin Solid Films 446 (2004) 138–142.
[27] W.J. Xu, T.S. Li, G.L. Zeng, F.F. Ren, S.H. Zhang, Y.J. Wu, T. Miyashita, Molecular arrangement and photopatterning of copolymer containing ketal-protected group in ultrathin nanosheets, Surf. Sci. 602 (2008) 1141–1148.
[28] W.J. Xu, T.S. Li, G.L. Zeng, S.H. Zhang, W. Shang, Y.J. Wu, T. Miyashita, Studies on photolithography and photoreaction of copolymer containing naphthyl in ultrathin nanosheets induced by deep UV irradiation, J. Photochem. Photobiol. A: Chem. 194 (2008) 97–104.
[29] G. Pohlers, J.C. Scaiano, R. Sinta, A novel photometric method for the determination of photoacid generation efficiencies using benzothiazole and xanthene dyes as acid sensors, Chem. Mater. 9 (1997) 3222–3230.
[30] W.J. Xu, F.F. Ren, S.H. Zhang, G.L. Zeng, T.S. Li, Y.J. Wu, Surface behavior of polymer Langmuir monolayer at the air/water interface, Adv. Technol. Mater. Mater. Proc. J. 8 (2006) 160–165.